

Electronic Supplementary Information

A polyoxometalate-based Pd^{II}-coordinated ionic solid catalyst for heterogeneous aerobic oxidation of benzene to biphenyl

Pingping Zhao,^a Yan Leng,^b Mingjue Zhang,^a Jun Wang,^{*a} Yajing Wu,^a and Jun Huang^a

^a *State Key Laboratory of Materials-Oriented Chemical Engineering, College of Chemistry and Chemical Engineering, Nanjing University of Technology, Nanjing 210009, China.*

^b *School of Chemical and Material Engineering, Jiangnan University, Wuxi 214122, China.*

** Corresponding author. Tel: +86-25-83172264; E-mail: junwang@njut.edu.cn*

1. General methods and materials

All chemicals were analytical grade and used as received. FT-IR spectra were recorded on a Nicolet 360 FT-IR instrument (KBr discs) in the 4,000–400 cm⁻¹ region. ¹H NMR spectra were measured with a Bruker DPX 300 spectrometer at ambient temperature in D⁶-DMSO using TMS as internal reference. ¹³C NMR spectrum was measured with a Bruker DPX 500 spectrometer at ambient temperature in D⁶-DMSO using TMS as internal reference. Electrospray ionization mass spectrum (ESI-MS) was recorded with a Finnigan mat APISQ 710 mass spectrometer. Elemental analyses were performed on a CHN elemental analyzer (FlashEA 1112). The amount of leached palladium species in the filtrate after a reaction was measured using a Jarrell-Ash 1100 ICP-AES spectrometer. ESR spectra were recorded on a Bruker EMX-10/12 spectrometer at X-band. The measurements were done at -110 °C in a frozen solution provided by a liquid/gas nitrogen temperature regulation system

controlled by a thermocouple located at the bottom of the microwave cavity within a Dewar insert. Solid UV-vis spectra were examined with a PE Lambda 950 spectrometer, and BaSO₄ was used as an internal standard. XRD patterns were collected on the Bruker D8 Advance powder diffractometer using Ni-filtered Cu K α radiation source at 40 kV and 20 mA, from 5 to 50 ° with a scan rate of 2 °/min, and before measurements the samples were dried at 100 °C for 2 h. SEM image was performed on a HITACHI S-4800 field-emission scanning electron microscope. BET surface areas were calculated from the sorption isotherms measured at the temperature of liquid nitrogen using a Micromeritics ASAP2010 analyzer. The samples were degassed at 150 °C to a vacuum of 10⁻³ Torr before analysis. TG analysis was carried out with a STA409 instrument in dry air at a heating rate of 10 °C/min.

2. Preparation of catalysts

H₅PMo₁₀V₂O₄₀ (H₅PMoV₂): The Keggin-structured double V-containing POM was prepared according to the procedure described in our previous report (*Y. Leng, H. Ge, C. Zhou, and J. Wang, Chem. Eng. J. 2008, 145, 335*). The detail of the preparation procedure is as the following. MoO₃ (16.59 g) and V₂O₅ (2.1 g) were added to deionized water (250 mL). The mixture was heated up to the reflux temperature under vigorously stirring with a water-cooled condenser, then at 120 °C the 85 wt% aqueous solution of H₃PO₄ (1.33 g) was added drop-wise to the reaction mixture. When a clear orange-red solution appeared, it was cooled to room temperature. The orange-red powder H₅PMo₁₀V₂O₄₀ was obtained by evaporation of the solution to dryness, followed with re-crystallizing for purification. The single V-containing POM

H₄PMo₁₁VO₄₀ (H₄PMoV) was synthesized based on the similar procedures using MoO₃ (17.79 g), V₂O₅ (1.02 g) and 85 wt% aqueous solution of H₃PO₄ (1.29 g).

[N-butyronitrile pyridinium]Cl ([C₃CNpy]Cl): The nitrile-tethered ionic liquid was synthesized according to the previous literature (D. Zhao, Z. Fei, T. Geldbach, R. Scopelliti, and P. Dyson, *J. Am. Chem. Soc.* 2004, 126, 15876). A mixture of pyridine (7.90 g, 0.10 mol) and Cl(CH₂)₃CN (12.43 g, 0.12 mol) was stirred at 80 °C for 24 h under nitrogen atmosphere. Two phases were formed from the mixture at the end of the reaction. After cooled to room temperature, the upper phase was decanted, then, acetonitrile (100 mL) and activated carbon (3.0 g) were added to the lower phase with a stirring for 30 min. The solution was then reheated to 80 °C and filtered. The resulting product was crystallized upon cooling to 0 °C, washed with diethyl ether for three times, and dried under vacuum for 24 h to afford ([C₃CNpy]Cl) as a colorless solid (yield: 90%). The other two ILs 1-Butyronitrile-3-methylimidazolium chloride ([C₃CNmim]Cl) (yield: 92%) and Butyronitrile-trimethylammonium chloride ([C₃CNTMA]Cl) (yield: 86%), were prepared accordingly.

[N-butyronitrile pyridinium]₄HPMo₁₀V₂O₄₀ ([C₃CNpy]₄HPMoV₂): The obtained IL [C₃CNpy]Cl (1.83 g, 0.01 mol) and H₅PMo₁₀V₂O₄₀ (3.47 g, 0.002 mol) were orderly added to 80 mL water, followed by a further stirring at room temperature for 24 h. Water was removed in vacuum to give the solid product. [C₃CNmim]₄HPMoV₂, [C₃CNTMA]₄HPMoV₂, and [C₃CNpy]₄PMoV₁ (PMoV₁: PMo₁₁V₁O₄₀⁴⁻) were prepared based on the similar procedures using corresponding precursors.

[(N-butyronitrile pyridinium)₂Pd(OAc)₂]₂HPMo₁₀V₂O₄₀

$[(C_3CNpy)_2Pd(OAc)_2]_2HPMoV_2$: $[C_3CNpy]_4HPMoV_2$ (0.5 mmol) was dissolved in 30 mL DMF, to which palladium acetate $Pd(OAc)_2$ (1 mmol) was added, and then the mixture was stirred at 70 °C for 12 h under nitrogen atmosphere. After filtration, the resulting brown solid was washed with DMF for three times, and dried in a vacuum oven at 80 °C for 12 h to give the final solid product. $[(C_3CNpy)_2Pd(OAc)_2]_2PMoV_1$, $[(C_3CNTMA)_2Pd(OAc)_2]_2HPMoV_2$ and $[(C_3CNmim)_2Pd(OAc)_2]_2HPMoV_2$ were synthesized according to same procedures using the corresponding precursors, respectively. $[(C_3CNpy)_2PdCl_2]_2HPMoV_2$ was prepared by reacting $[C_3CNpy]_4HPMoV_2$ with $PdCl_2$ with the stoichiometric molar ratio of 1:2.

3. Procedures for the aerobic coupling of benzene

The direct oxidative coupling reaction of benzene with molecular oxygen was carried out in a 100 mL pressured Parr-5500 stainless steel reactor with a mechanical stirrer. Typically, 0.12 g (0.043 mmol) catalyst $[(C_3CNpy)_2Pd(OAc)_2]_2HPMoV_2$, 30 mmol benzene were successively added into aqueous solution of acetic acid (10 mL, 67 vol%). After the system was carefully flushed with O_2 , the reactor was charged with 3 atm O_2 , heated to 100 °C and stirred at 800 r/min for 7 h. The reaction products were extracted by the mixed extractant of H_2O and CH_2Cl_2 (1:1). The extracted solution was analyzed by gas chromatography (SP-6890A) equipped with a FID detector and a capillary column (SE-54 30 m × 0.32 mm × 0.3 μm). Acetylacetone was used as the internal standard. Yield for biphenyl = $2 \times \text{mmol biphenyl} / \text{mmol initial benzene}$. Selectivity for biphenyl = $2 \times \text{mmol biphenyl} / (2 \times \text{mmol biphenyl} + \text{mmol phenol} + 3 \times \text{mmol terphenyls})$. The solid hybrid catalyst

$[(C_3CNpy)_2Pd(OAc)_2]_2HPMoV_2$ was recovered by filtration, washing with ethanol and drying in vacuum oven at 80 °C for 8 h. The catalytic performance of the recovered catalyst was tested under the above typical conditions.

Influences of various conditions on catalytic performances of $[(C_3CNpy)_2Pd(OAc)_2]_2HPMoV_2$ were investigated by respectively changing the catalyst amount, volume ratio of acetic acid to water in the solvent (aqueous solution of acetic acid), O₂ pressure, reaction time, and reaction temperature.

4. Characterizations of the synthesized hybrids

$[C_3CNpy]_4HPMoV_2$: Yield: 96%. Elemental analysis Calcd: C, 18.45 wt%; N, 4.78 wt%; H, 2.73 wt%. Found: C, 18.52 wt%; N, 4.83 wt%; H, 2.74 wt%. FI-IR (ν, KBr): 3447, 2248, 1075, 1055, 946, 872, 795 cm⁻¹. ¹H NMR (300 MHz, D⁶-DMSO, TMS); δ 9.110 (d, 2H), 8.644 (t, 1H), 8.228 (t, 2H), 4.727 (t, 2H), 2.653 (t, 2H), 2.320 (m, 2H). ¹³C NMR (500 MHz, D⁶-DMSO, TMS); δ 145.8, 144.9, 128.3, 119.4, 59.7, 26.3, 13.4. ESI-MS (D⁶-DMSO), positive ion m/z = 147 $[C_3CNpy]^+$. Negative-ion ESI-MS showed a fragmentation pattern identical to that of $HPMo_{10}V_2O_{40}^{4-}$, which is suggested to be an artifact of the electron spray ionization method (J. Ettetdgui, and R. Neumann., *J. Am. Chem. Soc.*, **2009**, 131, 4). The following assignments of the clusters are made: $PVMo_{10}O_{35}/2$ for m/z = 799; $PMo_9O_{29}/2$ for m/z = 681; $PVMo_8O_{29}/2$ for m/z = 656; $HV_2Mo_2O_{12}$ for m/z = 487; $Mo_4O_{13}/2$ for m/z = 296.

$[C_3CNpy]_4PMoV_1$: Yield: 93%. Elemental analysis Calcd: C, 19.15 wt%; N, 4.06 wt%; H, 2.03 wt%. Found: C, 19.21 wt%; N, 4.09 wt%; H, 2.08 wt%. FI-IR (ν, KBr): 3442, 2248, 1074, 1059, 967, 860, 777 cm⁻¹. ¹H NMR (300 MHz, D⁶-DMSO, TMS);

δ 9.114 (d, 2H), 8.644 (t, 1H), 8.225 (t, 2H), 4.727 (t, 2H), 2.653 (t, 2H), 2.320 (m, 2H).

$[\text{C}_3\text{CNmim}]_4\text{HPMoV}_2$: Yield: 94%. Elemental analysis Calcd: C, 14.63 wt%; N, 7.31 wt%; H, 2.66 wt%. Found: C, 14.77 wt%; N, 7.21 wt%; H, 2.73 wt%. FI-IR (ν , KBr): 3452, 2249, 1076, 1055, 947, 869, 798 cm^{-1} . ^1H NMR (300 MHz, D^6 -DMSO, TMS); δ 9.114 (s, 1H), 7.845 (d, 1H), 4.283 (t, 1H), 3.875 (t, 2H), 3.384 (b, 3H), 2.569 (m, 2H), 2.154 (m, 2H).

$[\text{C}_3\text{CNTMA}]_4\text{HPMoV}_2$: Yield: 98%. Elemental analysis Calcd: C, 14.99 wt%; N, 5.0 wt%; H, 2.72 wt%. Found: C, 15.08 wt%; N, 5.13 wt%; H, 2.74 wt%. FI-IR (ν , KBr): 3447, 2248, 1074, 1056, 947, 869, 798 cm^{-1} . ^1H NMR (300 MHz, D^6 -DMSO, TMS); δ 3.404 (m, 2H), 3.129 (s, 9H), 2.667 (t, 2H), 2.099 (m, 2H).

$[(\text{C}_3\text{CNpy})_2\text{Pd}(\text{OAc})_2]_2\text{HPMoV}_2$: Yield: 63%. BET surface area: 8.8 $\text{m}^2\cdot\text{g}^{-1}$. Elemental analysis Calcd: C, 19.07 wt%; N, 4.04 wt%; H, 2.06 wt%. Found: C, 19.02 wt%; N, 3.96 wt%; H, 2.00 wt%. FI-IR (ν , KBr): 3452, 2325, 1076, 1062, 1048, 941, 862, 793 cm^{-1} .

$[(\text{C}_3\text{CNpy})_2\text{Pd}(\text{OAc})_2]_2\text{PMoV}_1$: Yield: 68%. BET surface area: 9.3 $\text{m}^2\cdot\text{g}^{-1}$. Elemental analysis Calcd: C, 18.76 wt%; N, 3.98 wt%; H, 2.02 wt%. Found: C, 18.80 wt%; N, 3.98 wt%; H, 2.11 wt%. FI-IR (ν , KBr): 3452, 2326, 1074, 1060, 1046, 943, 865, 792 cm^{-1} .

$[(\text{C}_3\text{CNTMA})_2\text{Pd}(\text{OAc})_2]_2\text{HPMoV}_2$: Yield: 66%. BET surface area: 9.3 $\text{m}^2\cdot\text{g}^{-1}$. Elemental analysis Calcd for $[(\text{C}_3\text{CNpy})_2\text{Pd}(\text{OAc})_2]_2\text{PMoV}_1$: C, 16.07 wt%; N, 4.17 wt%; H, 2.71 wt%. Found: C, 16.14 wt%; N, 4.22 wt%; H, 2.82 wt%. FI-IR (ν , KBr):

3453, 2324, 1071, 1060, 1050, 943, 865, 796 cm^{-1} .

$[(\text{C}_3\text{CNmim})_2\text{Pd}(\text{OAc})_2]_2\text{HPMoV}_2$: Yield: 76%. BET surface area: 9.6 $\text{m}^2\cdot\text{g}^{-1}$.

Elemental analysis Calcd: C, 15.74 wt%; N, 6.12 wt%; H, 2.66 wt%. Found: C, 15.77 wt%; N, 6.21 wt%; H, 2.73 wt%. FI-IR (ν , KBr): 3452, 2324, 1072, 1060, 1048, 942, 866, 793 cm^{-1} .

$[(\text{C}_3\text{CNpy})_2\text{PdCl}_2]_2\text{HPMoV}_2$: Yield: 69%. BET surface area: 8.4 $\text{m}^2\cdot\text{g}^{-1}$. Elemental analysis Calcd: C, 16.15 wt%; N, 4.19 wt%; H, 2.43 wt%. Found: C, 16.23 wt%; N, 4.21 wt%; H, 2.54 wt%. FI-IR (ν , KBr): 3452, 2325, 1076, 1061, 1047, 941, 862, 793 cm^{-1} .

5. Supplementary Figures and Scheme

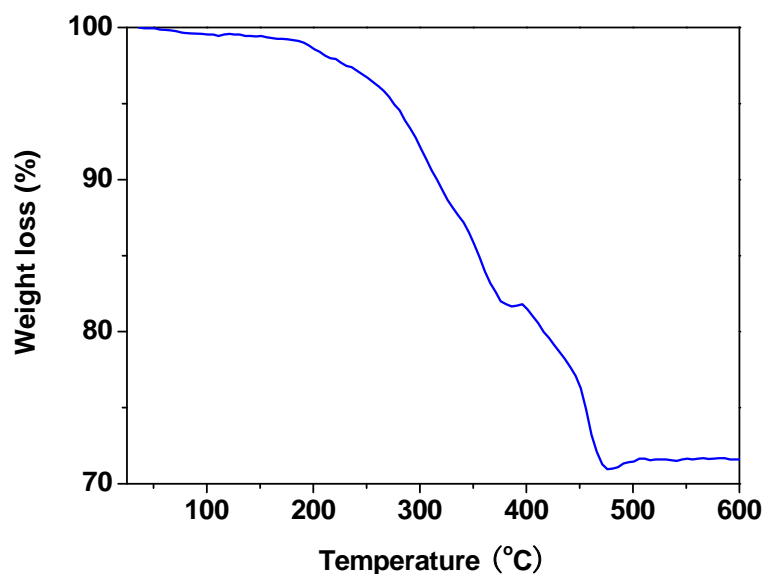


Fig. S1. TG curve of $[(\text{C}_3\text{CNpy})_2\text{Pd}(\text{OAc})_2]_2\text{HPMoV}_2$

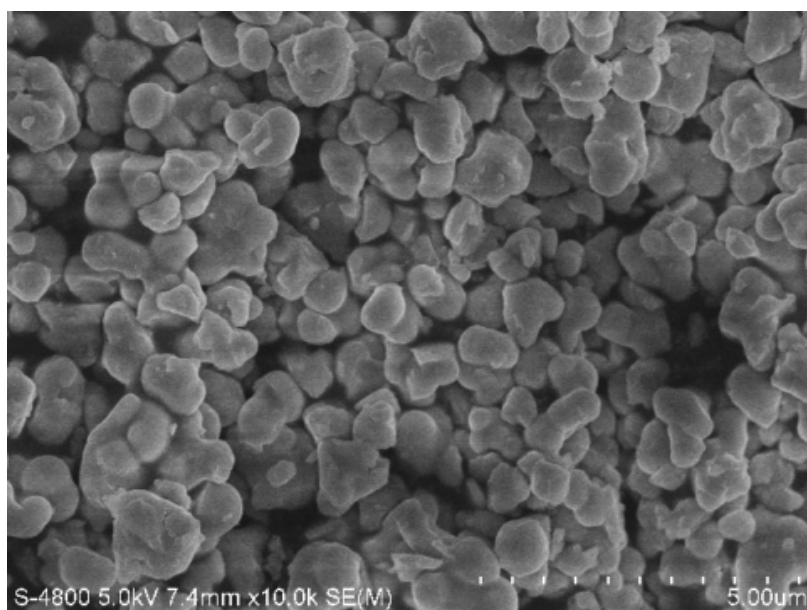


Fig. S2. SEM image of $[(C_3CNpy)_2Pd(OAc)_2]_2HPMoV_2$

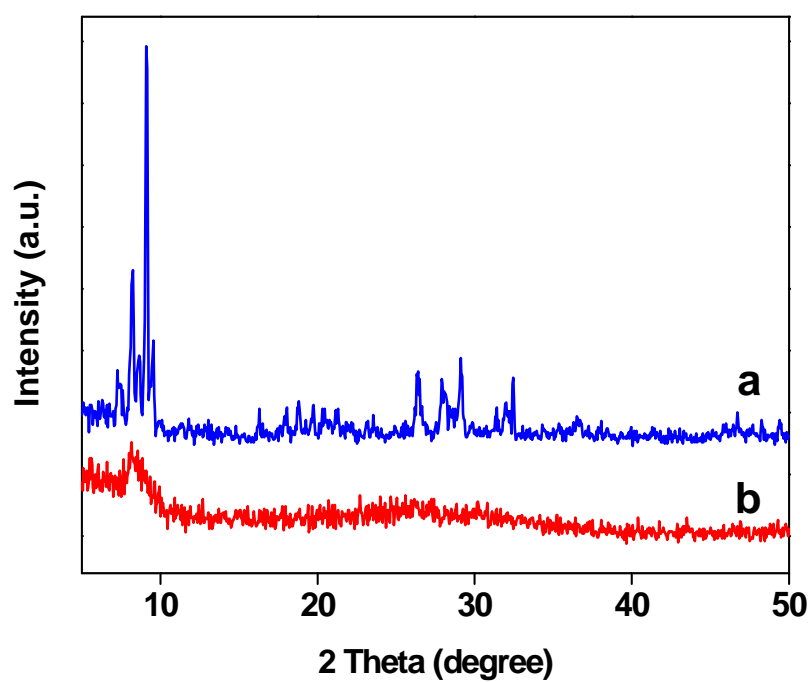


Fig. S3. XRD patterns of (a) $H_5PMo_{10}V_2O_{40}$ and (b) $[(C_3CNpy)_2Pd(OAc)_2]_2HPMoV_2$

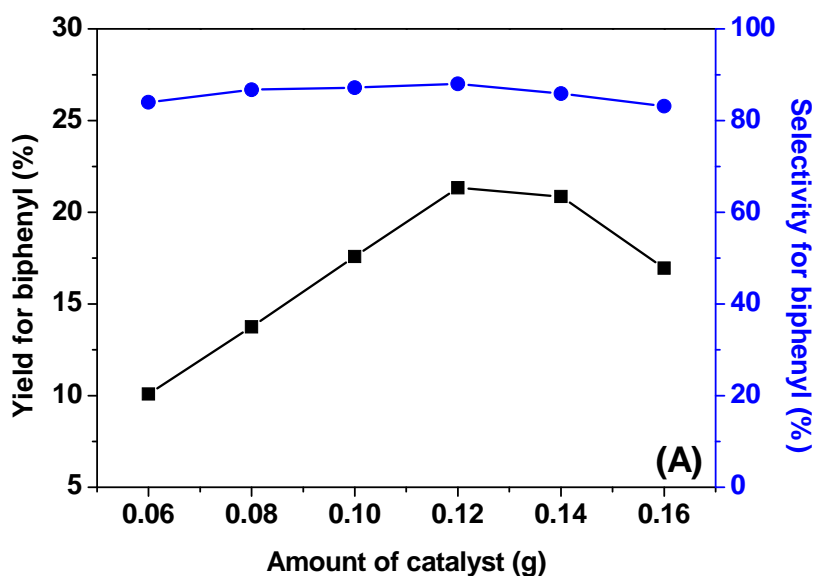


Fig. S4(A). Influence of catalyst amount on the direct oxidative coupling reaction of benzene with O₂ over the hybrid catalyst [(C₃CNpy)₂Pd(OAc)₂]₂HPMoV₂.

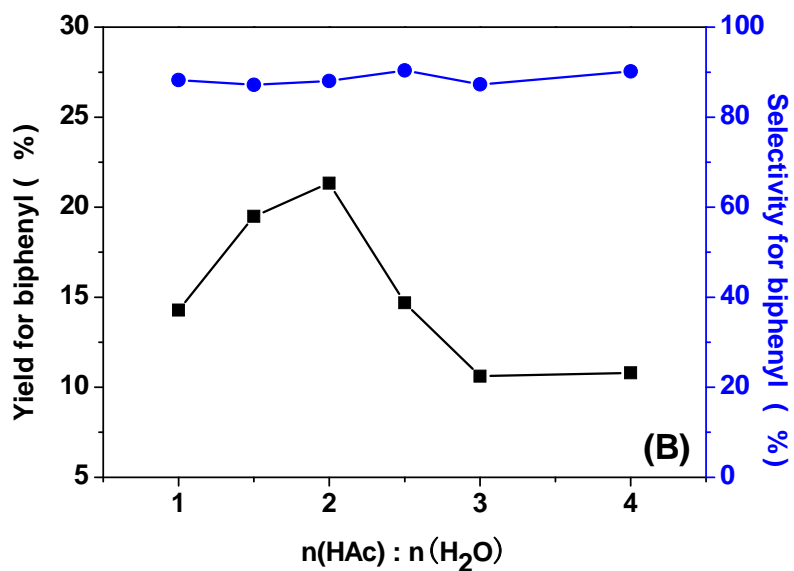


Fig. S4(B). Influence of volume ratio of acetic to water in the solvent on the direct oxidative coupling reaction of benzene with O₂ over the hybrid catalyst



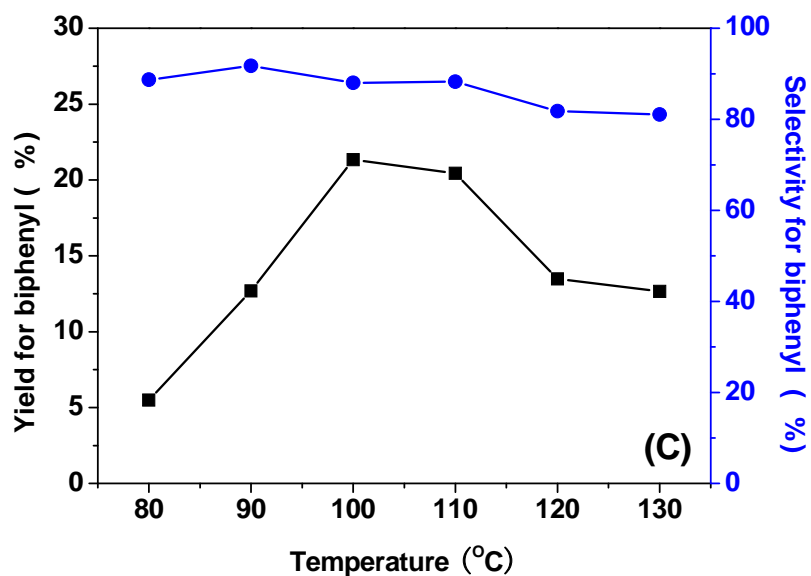


Fig. S4(C). Influence of reaction temperature on the direct oxidative coupling reaction of benzene with O₂ over the hybrid catalyst [(C₃CNpy)₂Pd(OAc)₂]₂HPMoV₂.

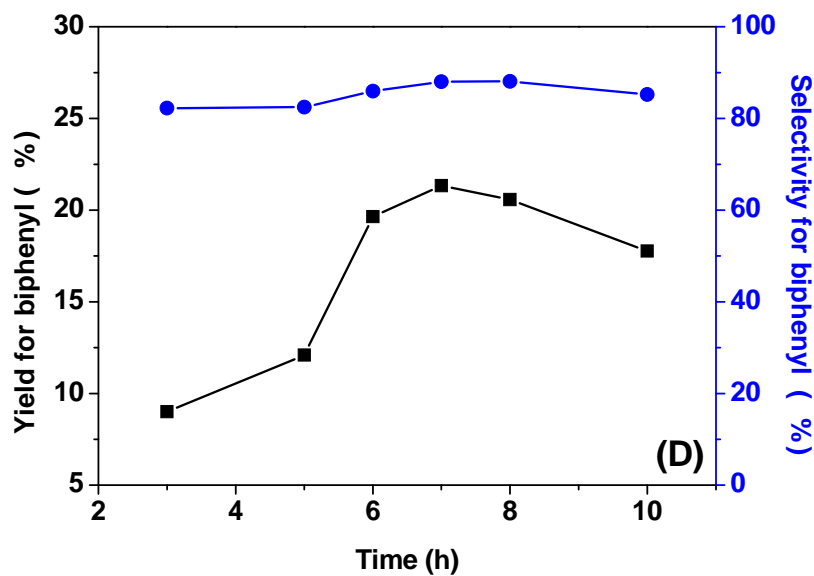


Fig. S4(D). Influence of reaction time on the direct oxidative coupling reaction of benzene with O₂ over the hybrid catalyst [(C₃CNpy)₂Pd(OAc)₂]₂HPMoV₂.

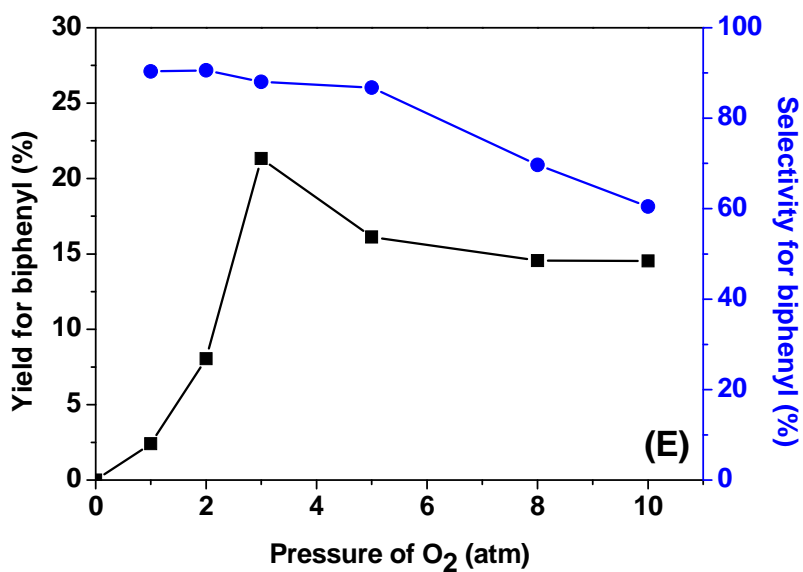


Fig. S4(E). Influence of O₂ pressure on the direct oxidative coupling reaction of benzene with O₂ over the hybrid catalyst [(C₃CNpy)₂Pd(OAc)₂]₂HPMoV₂.

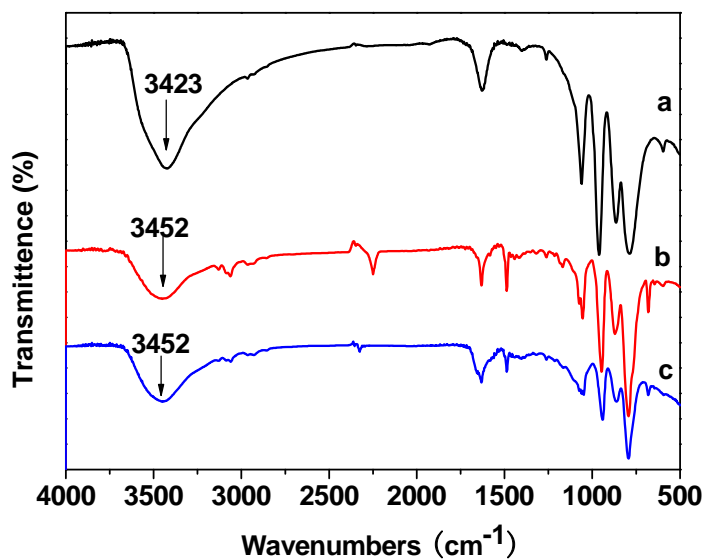


Fig. S5. IR spectra of (a) H₅PMo₁₀V₂O₄₀, (b) [C₃CNpy]₄HPMoV₂ and (c) [(C₃CNpy)₂Pd(OAc)₂]₂HPMoV₂

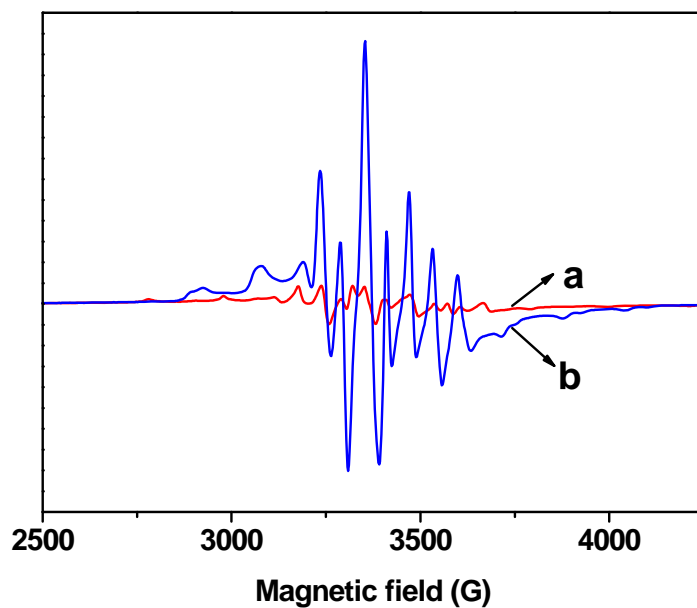


Fig. S6. ESR signals of (a) $[\text{C}_3\text{CNpy}]_4\text{HPMoV}_2$ and (b) $[(\text{C}_3\text{CNpy})_2\text{Pd}(\text{OAc})_2]_2\text{HPMoV}_2$

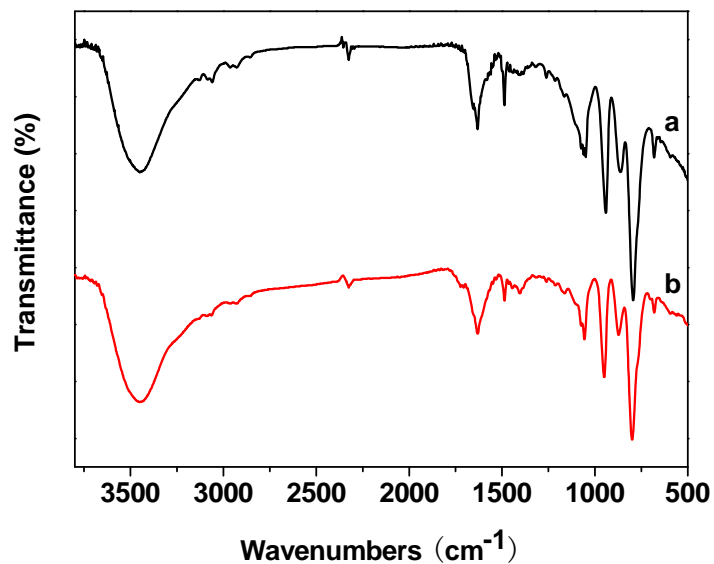
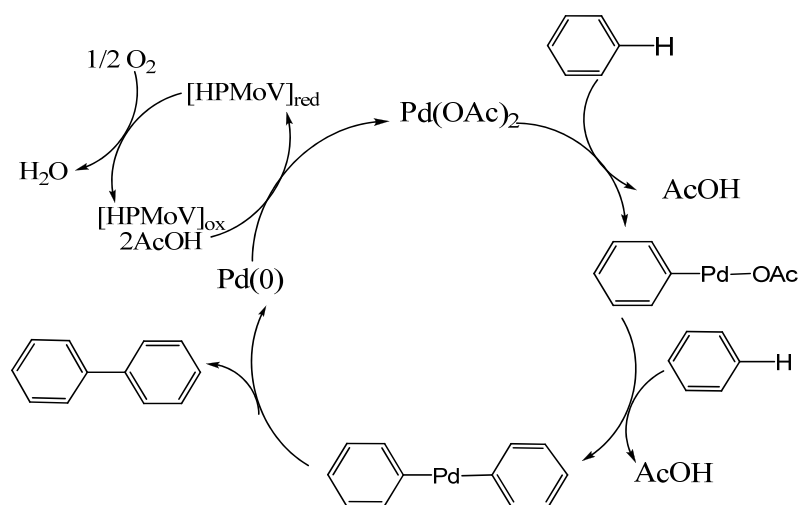


Fig. S7. IR spectra of (a) fresh $[(\text{C}_3\text{CNpy})_2\text{Pd}(\text{OAc})_2]_2\text{HPMoV}_2$ and (b) recycled $[(\text{C}_3\text{CNpy})_2\text{Pd}(\text{OAc})_2]_2\text{HPMoV}_2$



Scheme S1. Classical mechanism for the homogeneous aerobic benzene coupling process catalyzed individually by Pd(OAc)₂ and V-containing POM. (*J. E. Lyons, in: Oxygen Complexes and Oxygen Activation by Transition Metal Complexes, (Eds.: A.E. Martell, D. T. Sawyer), Plenum Press, New York, 1988, pp. 233-251)*)